Proc. Estonian Acad. Sci. Eng., 2006, **12**, 3-2, 284–299

An analysis of critical parameters of SiC JBS structures

Raido Kurel[a], Toomas Rang[a] and Laurent Poirier[b]

[a] Department of Electronics, Tallinn University of Technology, Ehitajate tee 5, 19086 Tallinn, Estonia; raido@elin.ttu.ee
[b] Faculty of Science and Technology, University of Nantes, 2 Rue de la Houssinière, 44322 Nantes Cedex3, France

Received 15 May 2006, in revised form 24 July 2006

Abstract. The paper presents the results of simulation and analysis of the critical parameters for SiC-based JBS devices. The inner processes of JBS have been investigated to get a better understanding of the main parameters inside the JBS device. The parameters that can not be measured by traditional techniques have the biggest impact on the electrical characteristics of the device. The best crystal polytype (4H- versus 6H-SiC) and workforce of Schottky contact metal are found for power application of the JBS.

Key words: Schottky interfaces, JBS structures, SiC, electrical characteristics, current crowding, numerical simulation.

1. INTRODUCTION

Silicon carbide is an outstanding compound semiconductor material with good physical properties. This makes it an excellent candidate for high speed and high temperature power electronic applications. Metal–semiconductor interface is one of the fundamental blocks in any semiconductor device technology. Furthermore, the 4H- and 6H-polytypes of SiC have some substantially different parameters, which have direct influence on the characteristics of the device.

Different barrier heights strongly influence the current transport in Schottky interfaces [1,2]. There are many aspects in simple Schottky devices, which are similar to those in JBS (e.g. the current crowding phenomenon). From another point of view, JBS devices have specific advantages compared to traditional simple *pn*- or Schottky devices. Many experimental results, dealing with the simulation of JBS devices, have been published [3–8]. Almost all simulation reports have investigated the relation of *pn*- and Schottky areas, only some papers deal with different Schottky contact metals, size and placing of implanted regions, and with thickness and doping concentration of the drift region. No papers have been published about JBS devices based on the *p*-type SiC. The processes inside JBS devices have been inadequately studied. The electric field strength distribution and minority carrier distribution in the device have been studied, although these studies have been concentrated only on certain parts inside the device in one dimension. In this paper we make an attempt to bridge this gap in some specific aspects.

The simulations have been done with simulation software SIC-DYNAMIT-2DT, earlier developed at the Department of Electronics of the TUT [9,10], aided by bash shell scripts for automation of simulations and gnu plot for presenting the results.

2. DESCRIPTION OF THE DEVICE

The detailed description of the model used here is presented in [11] and therefore it will not be discussed here in detail. Choosing the "best practice" geometric dimensions for the JBS device will be discussed in greater detail. Relevant simulation results are compared to find an optimum combination for power application: a device with low power losses, high reverse breakdown voltage and fast turn-off characteristic. The solution leads to optimal dimensions, which give best forward, reverse and turn-off characteristics. Firstly, the forward characteristic will be discussed (Fig. 1).

The simulations clearly show that devices with wider emitter have worse forward characteristics, especially in the low voltages region. The current density distribution along the x and y axes under small forward voltage for wide emitters ("1.5-10-1") is similar. The forward characteristic itself is not suitable for taking into account the demands to find the optimum combination for power application. The slope of the characteristic does not support the task to find the optimum. The explanation can be easily deducted from Fig. 2, where the electron concentrations inside the device are shown.

In case of a "slim" emitter ("1.5-10-0.5") the situation starts to change. The forward characteristic moves to the region, where the possibility to find the optimum increases significantly. The current density distributions shown in Fig. 3 explain the situation in detail.

The *x* component of the total current density reveals that the majority of the total current flows through the *pn*-part of the device. There is a little swing of the current towards the Schottky part of the device under emitter region, but a few micrometers above it even bigger swing of the current takes place in the opposite direction. The fact that the Schottky part of the device is not conducting can be explained by the lack of free electrons under Schottky contact (Fig. 2). The length of the Schottky contact area (in our case 0.5 μm) is small enough so that the built-in voltage of the *pn*-junction forms a depletion region under the whole

Schottky device and eliminates most of free electrons. Therefore the functioning of the Schottky device, as a majority carrier device, is disturbed. The influence of the Schottky area on the whole device is higher at low voltages because JBS

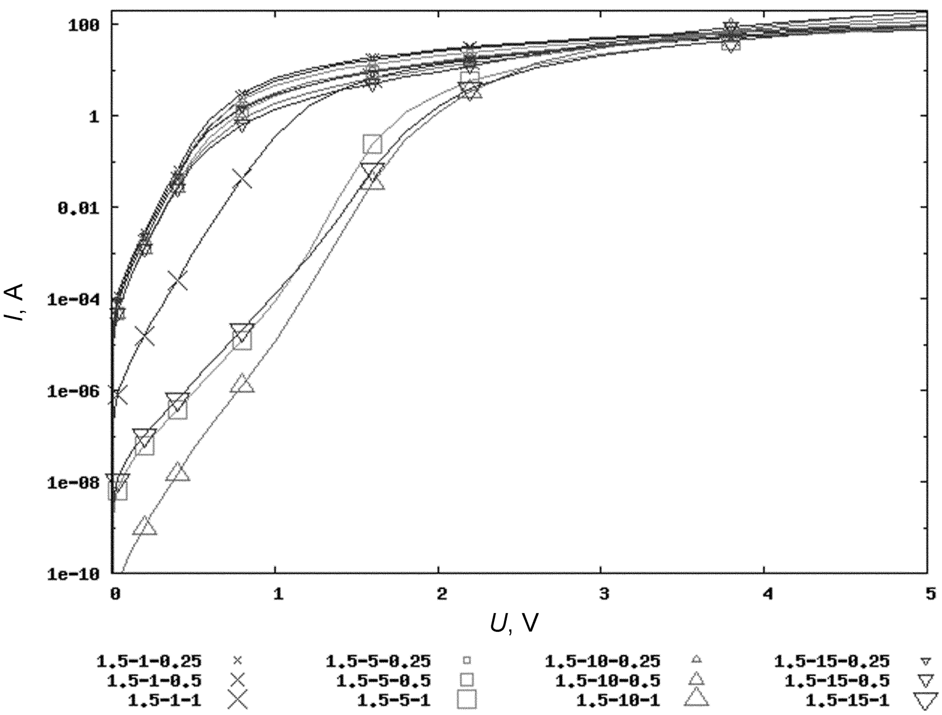

Fig. 1. Forward *U–I* characteristics of JBS devices with different deepness and width of the emitter area; legend shows width of the whole structure, deepness of the emitter and width of the emitter in μm.

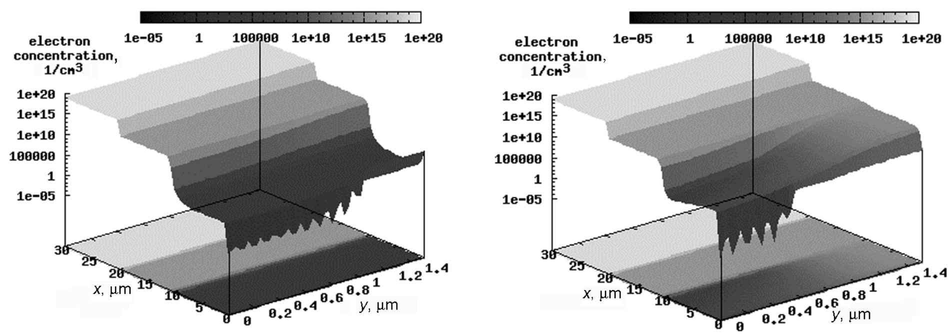

Fig. 2. Electron concentration in devices "1.5-10-1" (a) and "1.5-10-0.5" (b) for at 0.3 V forward voltage.

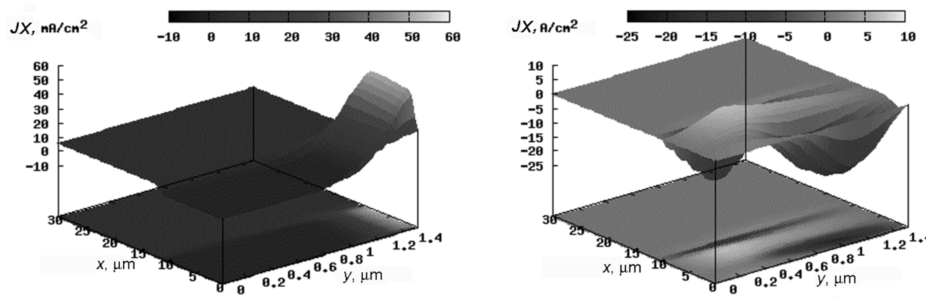

(a) (b)

Fig. 3. Values of the *x* (a) and *y* (b) components in the device “1.5-10-0.5” at 0.3 V forward voltage; direction of the current density is opposite to the direction of the *x* axis.

forward characteristics at low forward voltages are mostly determined by the Schottky area. By higher forward voltages the current flows through both parts of the device (Schottky and *pn*-interfaces). The influence of the Schottky part weakens. In case of wider Schottky area there is no lack of electrons any more (Fig. 2) and the majority of the current flows through the Schottky contact already at 0.3 V forward voltage (Fig. 3). Current swing to the Schottky part of the device takes place below the emitter area. There is another redistribution of the current in the opposite direction just below the surface. The concentration of electrons is higher in this particular area resulting in lower resistance and allowing easy current redistribution in horizontal direction under the Schottky barrier. The low current density (in *x* direction) region under Schottky contact near the emitter can be explained by the lack of electrons in this area. Current density distribution in *y* direction reveals that current swings away from the *pn*-part of the device under emitter and also in a small (few micrometers) region under the Schottky contact. There is a small region above the emitter, where the current flows towards the *pn*-part of the device.

Next the reverse characteristics are examined. Figure 4 shows that the characteristics do not differ sufficiently except in the case when the width of the emitter area is equal to 1 μm. Devices with narrow emitter area do not block the Schottky reverse leakage current. Reverse current of the device is flowing mostly through the Schottky part (Fig. 5). Crowding of the reverse leakage current to Schottky part is taking place in a specific place (bottom) of the epitaxial layer and current is redistributed under the Schottky contact. Devices with a wide emitter width are able to block effectively Schottky leakage current. In this case most of the reverse leakage current flows through the *pn*-part of the device.

There exist two regions, where reverse current swings to the *pn*-part of the device: the bottom of the epitaxial layer and the middle region of the emitter. We can see that part of the current swings back to Schottky region of the device in the upper half of the emitter region. This behaviour causes also a current peak in the emitter. All these phenomena are well explained with current distribution shown in Fig. 6.

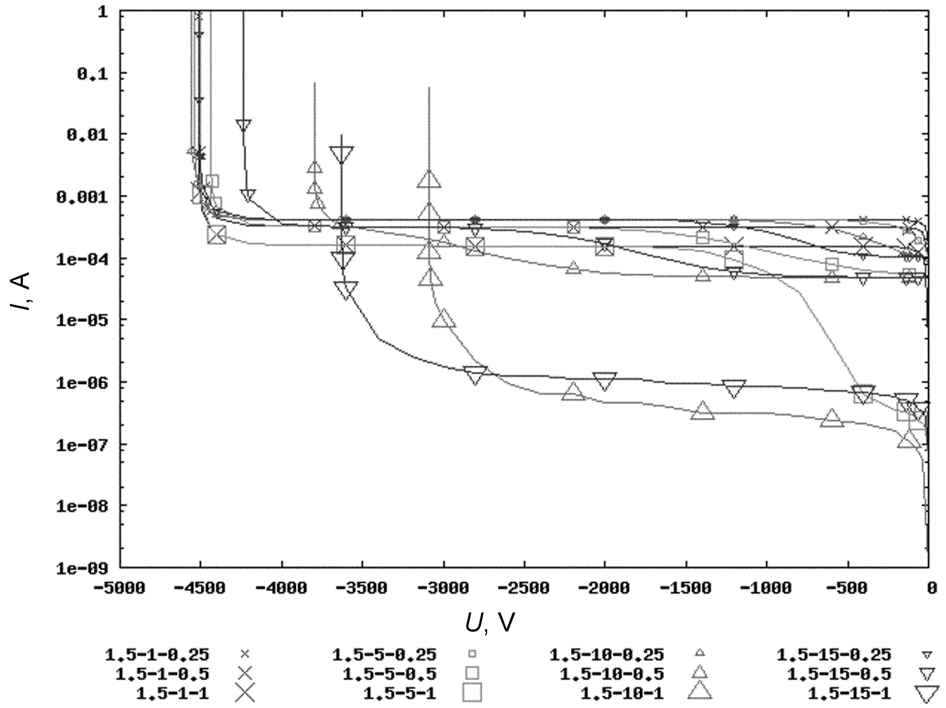

Fig. 4. Reverse *U–I* characteristics of JBS devices with different deepness and width of the *p* doping area; legend shows width of the whole structure and deepness and width of the *p* doping area in μm.

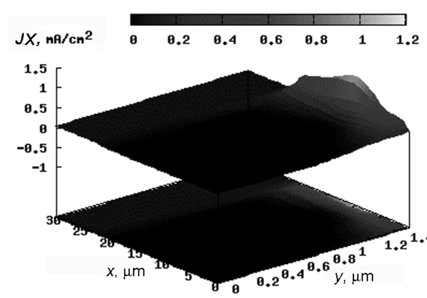

(a)

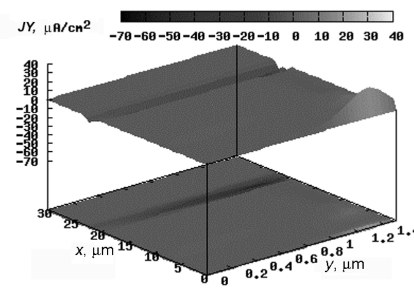

(b)

Fig. 5. Values of the *x* (a) and *y* (b) components of the density of the reverse current in the device “1.5-10-0.5” at 1000 V reverse voltage; current density direction is opposite to the direction of the *x* axis.

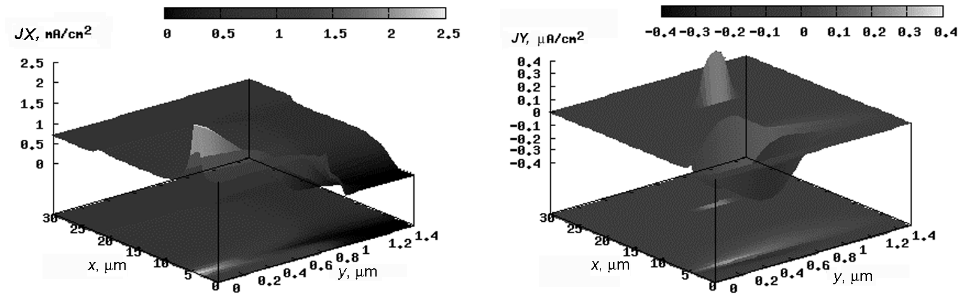

(a) (b)

Fig. 6. Values of the *x* (a) and *y* (b) components of the density of the reverse current in the device "1.5-10-1" at 1000 V reverse voltage; current density direction is opposite to the direction of the *x* axis.

The analysis of the distribution of the strength of the electric field is interesting and provides valuable information. Here we are faced with two aspects. Firstly, the maximum electric field strength inside the device should not be too high, because of limited ability of the semiconductor material to handle high electric field strengths. Secondly, the electric field strength under contact should be as low as possible to reduce the effect of lowering of the Schottky barrier. Lower electric field strength near the surface means also fewer problems in passivation technique of the device surface. The last moment is extremely important, as the proper passivation of the device surface can significantly decrease any kind of leakages caused by the strength of the electrical field. It is especially important in case of SiC, where the strength of the electric field reaches much higher values than in case of Si. The worst case stems from the solution, where the emitter depth is small (Fig. 7). In this particular situation the distribution of the electric field inside the device under Schottky contact matches pretty well that of a single Schottky diode. The strength of the electric field has highest value under the contact and decreases linearly over epitaxial layer until the substrate. This situation has, however, another disadvantage: maximum value of the field strength is extremely high and it is not located favourably (maximum value is under contact). Electric field distribution in case of a device with 10 μm deep and 0.5 μm wide emitter is shown on Fig. 8. Electric field distribution is quite similar in the Schottky and *pn*-part of the device. Maximum of the electric field strength is through the entire device below the emitter (at around $x = 11$ μm).

The turn-off characteristics (Fig. 9) show clearly that the devices with the lowest depth of the emitter have the most undesired parameters. This follows directly from the distribution and concentration of minority carriers. Deep emitter area introduces also the highest number of majority carriers, which are situated over a relatively large area. The distribution of hole concentration at forward voltage 5 V for the devices "1.5-10-0.5" and "1.5-1-0.5" is shown in Fig. 10.

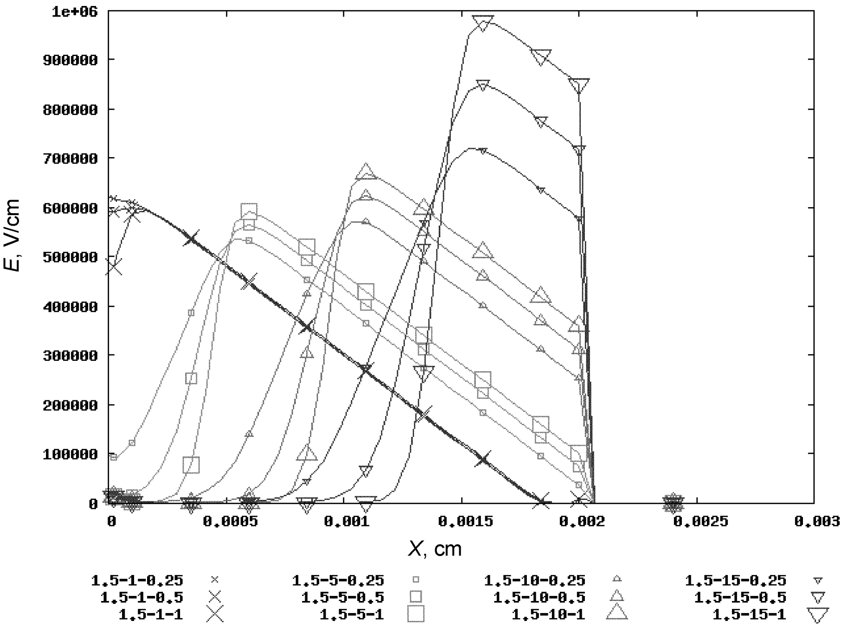

Fig. 7. Distribution of the electric field under Schottky contact of JBS devices with different emitter deepness and width; legend shows width of the whole structure and deepness and width of the emitter in μm.

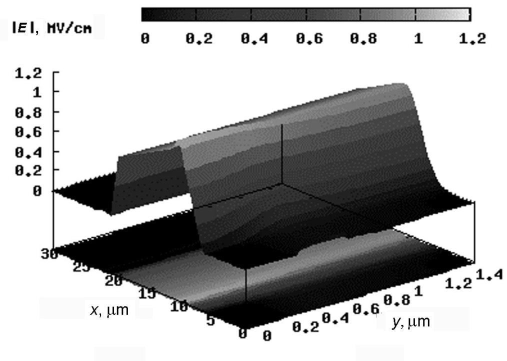

Fig. 8. Electric field distribution at reverse voltage 1000 V in case of the device “1.5-10-0.5”.

As seen in Figs. 9 and 10, the amount of holes needed to be carried out from the device depends strongly on the deepness of the emitter. The amount of electrons needed to be carried out during the turn-off process has strong influence also on the turn-off time. This is the main factor which determines the dependence of the turn-off time on emitter area dimensions.

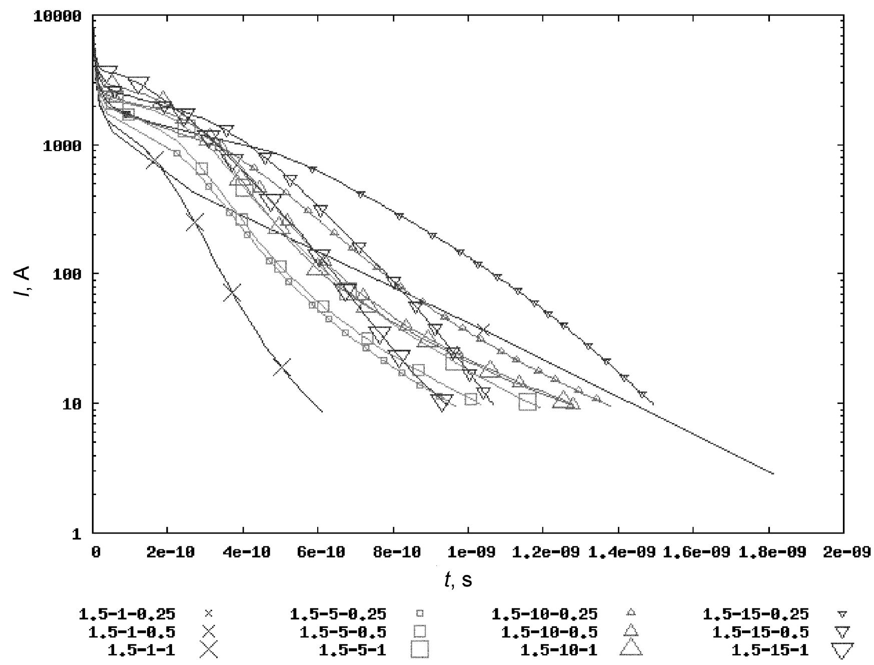

Fig. 9. Turn-off current switching JBS from 100 A to –100 V with different emitter deepness and width; legend shows width of the whole structure and deepness and width of the emitter in μm.

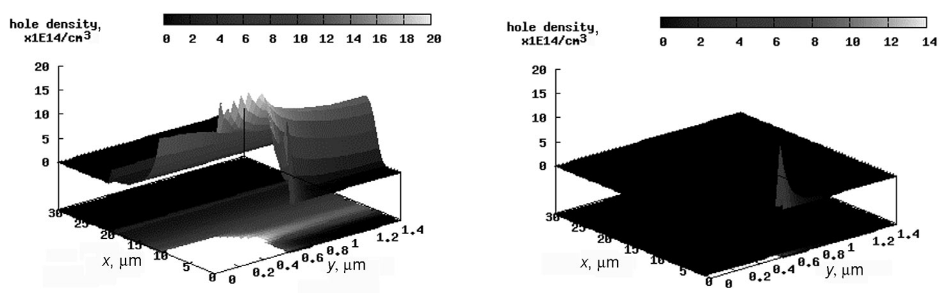

(a)

(b)

Fig. 10. Hole density at forward voltage 5 V: (a) device "1.5-10-0.5" (emitter area hole concentration is out of the range and not shown); (b) device "1.5-1-0.5".

Our simulations show that small width of the emitter prolongs the slope of turn-off characteristics, but large width of the emitter distorts the forward characteristics. Thus middle-scale dimensions should be chosen. The electric field strength both under the Schottky contact and in the bulk of the semiconductor should be chosen low in case of an emitter of average depth. There are no big differences whether the substrate material is 4H-SiC or 6H-SiC.

3. RESULTS AND DISCUSSION

Now we proceed to the investigation of the changes of forward, reverse, and turn-off characteristics, which is supported by the analysis of the distribution of the electric field strength.

3.1. Comparison of polytypes: 6H-SiC versus 4H-SiC

Our simulations show clearly that the current level at low voltages (below 0.4 V) for 6H-SiC devices is higher than for 4H-SiC devices under forward bias. The opposite situation is true for higher voltages (Fig. 11). Higher currents of 6H-SiC at low voltages can be explained by lower band gap of 6H-SiC compared to 4H-SiC. This results in lower voltage drop on Schottky barrier of Schottky part of the device. Still, this influence is seen only on low voltages because the resistance of the 6H-SiC semiconductor is higher than that of 4H-SiC due to much lower carrier mobility along the *c* axis in 6H-SiC. The reverse characteristics of 6H-SiC based devices have higher reverse current and higher breakdown voltage than the 4H-SiC based ones (Fig. 11). Higher reverse current is caused by the characteristics of the Schottky contact. The Schottky part of the device has higher leakage current under reverse voltage situation and this determines the reverse current for the whole device. Smaller values of reverse breakdown voltages are caused by lower breakdown electric field strength for 4H-SiC.

The turn-off characteristics (Fig. 12) show that the devices based on the 6H-SiC turn off during a longer time than the devices based on 4H-SiC. It is explained by the lower mobility of charge carriers in 6H-SiC. The electric field distribution (Fig. 12) has the same character for both materials. Comparison of 4H-SiC and 6H-SiC shows clearly that a substrate from 4H-SiC guarantees better characteristics in almost all aspects except in the values of breakdown voltages. The main reason for better performance of 4H-SiC is lower values of mobility of

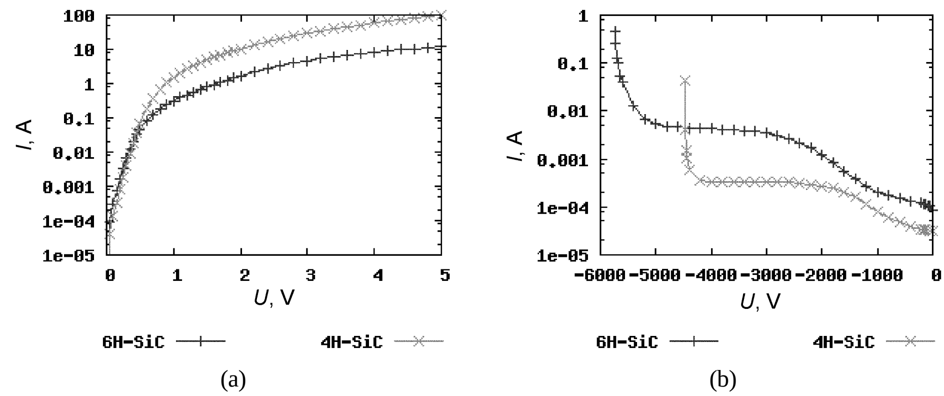

Fig. 11. Forward (a) and reverse (b) *U–I* characteristics of 6H-SiC and 4H-SiC.

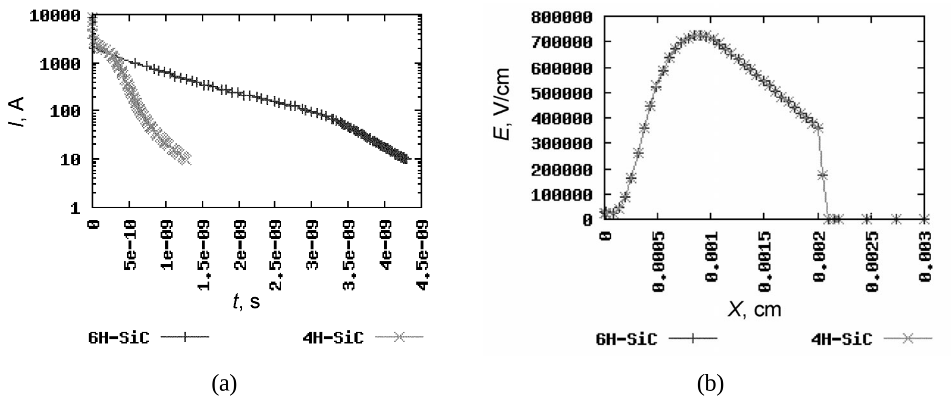

Fig. 12. The turn-off characteristics (a) and distribution of the electric field strength (b) in 6H-SiC and 4H-SiC JBS devices.

charge carriers compared to 6H-SiC, resulting in higher specific resistance. The smaller breakdown voltage is caused by lower breakdown electric field strength of 4H-SiC.

3.2. Variation of the doping concentration of the epitaxial layer

Doping concentration of the epitaxial layer influences the forward characteristics twofold (Fig. 13). Dependence of the Schottky junction characteristics on epitaxial layer concentration causes difference in the low voltage part of the forward characteristics. Change of the resistance of the epitaxial layer, caused by concentration change, is seen for higher voltages. Devices with higher concentration of the epitaxial layer have lower resistance and thus bigger current at the

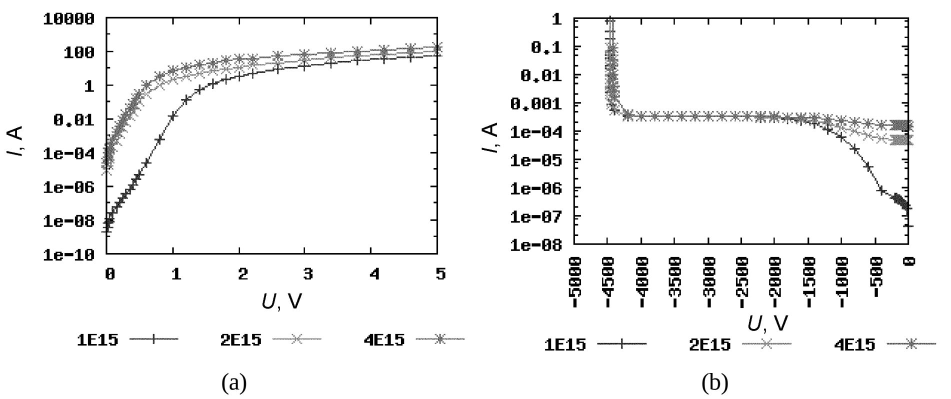

Fig. 13. Dependence of the forward (a) and reverse (b) characteristics on the doping concentration of the epitaxial layer.

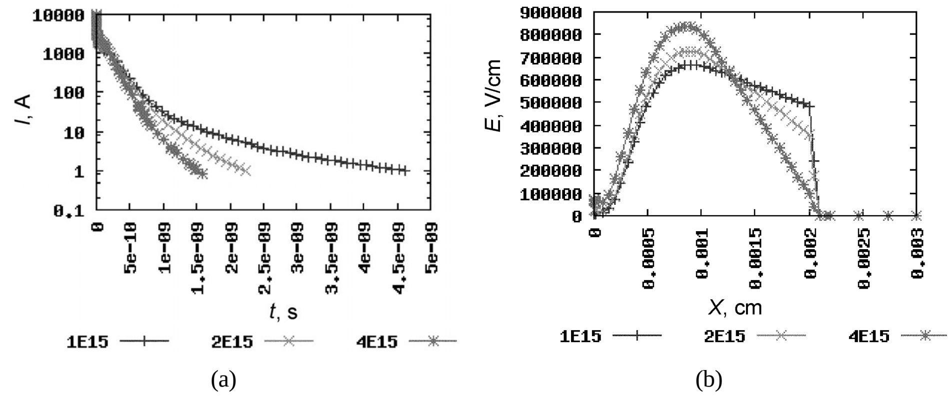

Fig. 14. Dependence of the turn-off characteristics (a) and electric field distribution (b) on the doping concentration of the epitaxial layer.

same voltage. On reverse bias the resistance of epitaxial layer is not important. By higher voltages, reverse characteristics are identical (Fig. 13). There is a difference by lower reverse voltages. The concentration of electrons under Schottky contact is low in case of low doping concentration of the epitaxial layer at low reverse voltages. The majority of current flows through the *pn*-part of the device. The concentration level of electrons is much higher in case of higher doping concentration of the epitaxial layer and leakage current of the Schottky part of the device determines the reverse leakage of the device.

The turn-off characteristics (Fig. 14) show that doping concentration of the lower epitaxial layer leads to devices with a longer turn-off time, which results from the higher resistance in the epitaxial region. The epitaxial layer concentration in turn has strong influence on the distribution of the electric field strength along the epitaxial layer (Fig. 14). The region, where the electric field is mostly influenced by epitaxial layer concentration, is below the emitter and above the highly doped substrate. By higher doping concentration of the epitaxial layer the slope of the electric field is sharper. As the device has to handle the same voltages, the integral of the electric field strength over the device must be the same. In case of a sharper slope, the distribution of electric field strength is less even, causing lower electric field strength region in the lower part of the epitaxial layer, but also higher electrical field strength near the bottom of the emitter. The highest strength of the electric field is important as the breakdown of the device depends on it.

3.3. Variation of the metal work function of the Schottky contact

In figures on forward characteristics it is seen that the metal work function has an influence in the lower voltage region, where characteristics are determined by the Schottky part of the device (Fig. 15). Lower Schottky barrier height causes higher currents in the low voltage region of the characteristic. By higher voltages, the characteristics of the Schottky part of the device are not so important any more. The forward *U–I* characteristics are similar, depending mostly on the behaviour of the *pn*-part of the device. The reverse characteristics of the device depend strongly on the contact metal work function, as leakage current of the Schottky part of the device determines the current leakage of the whole device (Fig. 15). Lower metal work function of the Schottky contact causes higher leakage currents in the Schottky part of the device and also in the device as a whole.

The turn-off characteristics (Fig. 16) do not depend on the value of the contact metal work function. The distribution of currents in reverse voltage situation is the same for all the three chosen work function values. Therefore also the turn-off characteristics do not depend on it. The electric field strength (Fig. 16) does not depend on the metal work function value of the Schottky contact either. Barrier height of the Schottky contact has only small influence on the electric field just below the Schottky contact.

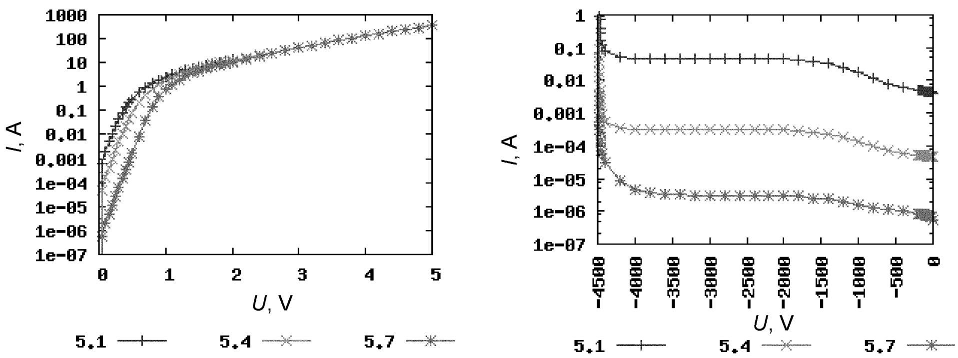

(a) (b)

Fig. 15. Dependence of the forward (a) and reverse (b) characteristics on the contact metal work function.

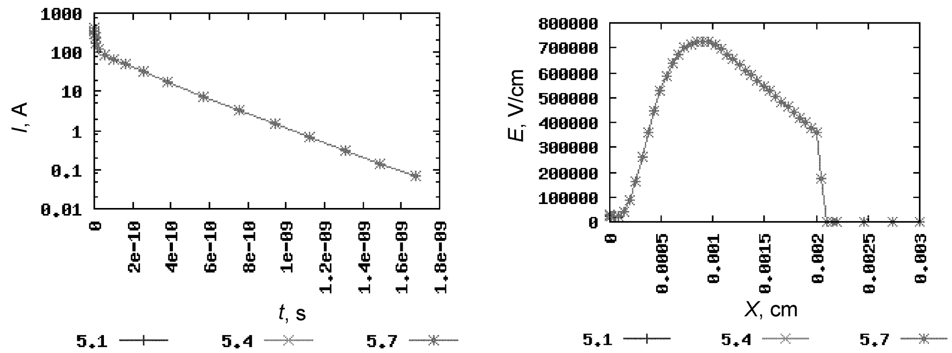

(a) (b)

Fig. 16. Dependence of the turn-off characteristics (a) and electric field strength distribution (b) on the contact metal work function.

3.4. Comparison of the Schottky, JBS and *pn*-diodes

Forward characteristic of the JBS device is between the Schottky and *pn*-diode, closer to the Schottky diode (Fig. 17). By lower forward voltages only Schottky part of the device conducts. The characteristics of the JBS device try to copy the characteristics of the best of the two. The difference in JBS and best characteristic (Schottky interface at low voltages and *pn*-junction at high voltages) is only caused by the area of the device, which conducts at the moment. If areas of the Schottky and *pn*-part of the JBS device are equal, the majority of current flows through the Schottky part, as it normally does in low voltages region. The current density of the whole device is about twice lower as could be expected, because the active area is twice smaller as well. Reverse characteristic of the JBS device is also between Schottky and *pn*-diode, close to Schottky diode (Fig. 17). In the ideal case, the JBS reverse current should be more like in a *pn*-diode because the depletion region cuts away the Schottky leakage current. In many applications of power devices the low reverse leakage is not as important as the high forward current. Reverse currents of the chosen best device are small enough not to cause remarkable self-heating of the device. Although both forward and reverse characteristics of the chosen best JBS device are close to those of the Schottky diode, the JBS device has other qualities superior to the latter. The dependence of the Schottky barrier height on applied voltage (Schottky effect) is not considered in this work. This effect would probably raise the reverse leakage current of Schottky diodes considerably, as the electric field strength under the Schottky contact is very high in case of a pure Schottky diode as compared to the JBS diode (Fig. 17). This means that reverse leakage current of the JBS diode is lower than that of the pure Schottky diode by high voltages. Besides the Schottky effect there is another very important effect. High electric field strength under surface means very difficult passivation tasks, which still probably will not allow such high electric field strengths as in the bulk of a

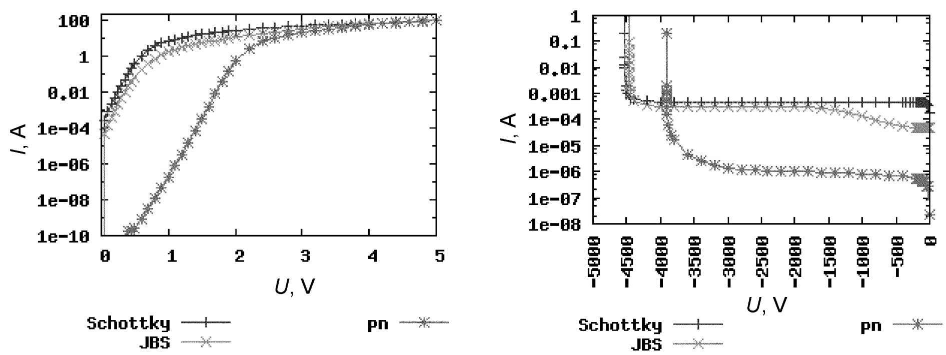

(a) (b)

Fig. 17. Forward (a) and reverse (b) characteristics of the Schottky, JBS and *pn*-diodes.

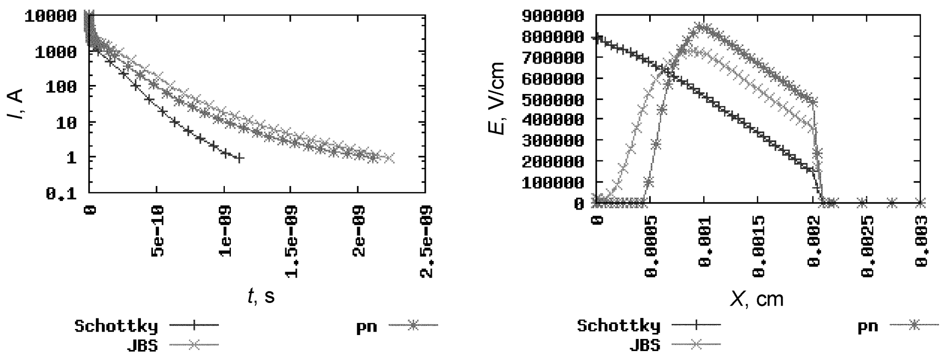

(a) (b)

Fig. 18. Distribution of the turn-off characteristics (a) and electric field strength (b) in Schottky, JBS and *pn*-diodes.

semiconductor. This simulation does not consider surface breakdown effects. The gain from JBS in real life is even more promising because of this fact.

Dependence of the electric field strength on the device type (Fig. 18) is most important. The effect of lowering of the electric field strength under Schottky contact can be seen. There is no such effect in the case of the pure Schottky device. The maximum electric field strength of JBS is lower than that of the *pn*-diode. This comparison is relative as unnaturally deep emitter is used compared to normal *pn*-diode acceptor implantation. This fact forces voltage of the *pn*-diode to drop in a considerably smaller area of *n*-type lower doped epitaxial layer than in a normal *pn*-diode. Still, if we consider devices with the same *p*-area, JBS device has lower maximum electric field strength and can sustain higher reverse voltage. The turn-off characteristic of the JBS device is close to that of the *pn*-device (Fig. 18). Although there is a parallel Schottky structure, high forward currents are still causing minority carrier accumulation in the epitaxial layer. Turn-off time of the JBS device is close to that of the Schottky devices and the device is switched off from low forward current. Almost all current flows through the Schottky device and there is very low minority carrier accumulation in the epitaxial layer.

4. CONCLUSIONS

Relevant simulation results of JBS devices have been presented. An analysis of the optimal combination for power JBS application has been performed. Preferable are devices with low power losses, high reverse breakdown voltage and fast turn-off characteristics. As the best device configuration for all the applications is never available, it is important that such a device is chosen that aims to reduce the need for complex passivation solutions by keeping electric field strength under surface very low.

The best *n*-substrate-based JBS device for power application was found as a result of the investigations. As for device dimensions, the so-called balanced middle size geometrical solution should be used. The 4H-SiC has significant advantages over the 6H-SiC solution. The concentration of the epitaxial layer and the metal work function values of the Schottky contact influence mostly the *U–I* characteristics of the JSB device and should be determined mainly on this basis.

ACKNOWLEDGEMENTS

The authors wish to thank the Estonian Science Foundation for the support of this research (grant No. 5901). We would also like to thank Dr. Andres Udal for developing SiC-DYNAMIT-2DT simulation software, used here as a simulating instrument.

REFERENCES

1. Kurel, R. and Rang, T. Ambient temperature influence on current suppressing effect caused by self-heating phenomenon at 6H-SiC Schottky interfaces. In *Proc. Baltic Electronics Conference BEC'98*. Tallinn, 1998. TTÜ Kirjastus, Tallinn, 1998, 253–254.
2. Kurel, R. and Rang, T. Self-heating phenomenon and current suppressing effect at 6H-SiC Schottky interfaces. In *Proc. 5th NEXUSPAN Workshop on Thermal Aspects in Micro-system Technology*. Budapest, 1998, 88–91.
3. Zhu, L., Shanbhag, M., Chow, T. P., Jones, K. A., Ervin, M. H., Shah, P. B., Derenge, M. A., Vispute, R. D., Venkatesan, T. and Agarwal, A. 1kV 4H-SiC JBS rectifiers fabricated using an AlN capped anneal. *Trans. Tech. Publ. Mater. Sci. Forum*, 2003, **433–436**, 843–846.
4. Singh, R., Capell, D. C., Hefner, A. R., Lai, J. and Palmour, J. W. High-power 4H-SiC JBS rectifiers. *IEEE Trans. Electron Devices*, 2002, **49**, 2054–2063.
5. Pérez, R., Mestres, N., Tournier, D., Jordà, X., Vellvehí, M. and Godignon, P. Temperature dependence of 4H-SiC JBS and Schottky diodes after high temperature treatment of contact metal. *Trans. Tech. Publ. Mater. Sci. Forum*, 2005, **483–485**, 945–948.
6. Asano, K., Hayashi, T., Saito, R. and Sugawara, Y. High temperature static and dynamic characteristics of 3.7 kV high voltage 4H-SiC JBS, power semiconductors devices and ICs. In *Power Semiconductor Devices and ICs, 2000. Proc. 12th International Symposium*. Toulouse, 2000, 97–100.
7. Rottner, K., Frischholz, M., Myrtveit, T., Mou, D., Nordgren, K., Henry, E., Hallin, C., Gustafsson, U. and Schöner, A. SiC power devices for high voltage applications. *Mater. Sci. Eng. B*, 1999, **61–62**, 330–338.
8. Ayalew, T., Kim, S. C., Grasser, T. and Selberherr, S. Numerical analysis of SiC merged PiN Schottky diodes. *Trans. Tech. Publ. Mater. Sci. Forum*, 2005, **483–485**, 949–952.
9. Udal, A. *Development of Numerical Semiconductor Device Models and their Application in Device Theory and Design*. Theses of Tallinn Technical Univ., TTÜ Kirjastus, Tallinn, 1998.
10. Kurel, R. and Udal, A. Two-dimensional nonisothermal analysis of current crowding effect at nonuniform SiC Schottky contacts using device simulator DYNAMIT-2DT. In *Proc. 8th Baltic Electronics Conference*. Tallinn, 2002. TTÜ Kirjastus, Tallinn, 2002, 51–54.
11. Kurel, R. and Rang, T. Static and dynamic behavior of the SiC complementary JBS structures. In *Proc. 10th Baltic Electronics Conference*. Tallinn, 2006. TTÜ Kirjastus, Tallinn, 2006.

SiC JBS-struktuuride kriitiliste parameetrite analüüs

Raido Kurel, Toomas Rang ja Laurent Poirier

On esitatud *pn*- ning Schottky siirdeid sisaldavate pooljuhtseadiste (JBS) simuleerimise tulemusi ja nende seadiste kriitiliste parameetrite analüüs. On uuritud JBS-struktuuride sisemisi parameetreid (elektrivälja tugevus, barjääri kõrgus jne), mis põhiliselt mõjutavad seadise elektriliste karakteristikute käitumist ega ole mōōdetavad traditsiooniliste meetoditega. On leitud parim lahendus JBS-struktuuridele, lähtudes kristalli polütüübist (4H- vōi 6H-polütüüp) ja Schottky kontakti metalli väljumistööst.